



HHS Public Access

Author manuscript

Acta Biomater. Author manuscript; available in PMC 2016 February 01.

Published in final edited form as:

Acta Biomater. 2015 February ; 13: 52–60. doi:10.1016/j.actbio.2014.11.012.

Photoinitiator-Free Synthesis of Endothelial Cell Adhesive and Enzymatically Degradable Hydrogels

Derek R. Jones¹, Roger E. Marchant¹, Horst von Recum¹, Anirban Sen Gupta¹, and Kandice Kottke-Marchant^{1,2,*}

¹Department of Biomedical Engineering, Case Western Reserve University, Cleveland, OH 44106, USA

²Robert J. Tomsich Pathology and Laboratory Medicine Institute, Cleveland Clinic, Cleveland, OH 44195, USA

Abstract

We report on a photoinitiator-free synthetic method of incorporating bioactivity into poly(ethylene glycol) (PEG) hydrogels in order to control physical properties, enzymatic biodegradability and cell-specific adhesiveness of the polymer network, while eliminating the need for UV-mediated photopolymerization. To accomplish this, hydrogel networks were polymerized using Michael addition with four-arm PEG acrylate (10 kDa), using a collagenase sensitive peptide (CSP) as a crosslinker, and introducing an endothelial cell adhesive peptide either terminally (RGD) or attached to the crosslinking peptide sequence (CSP-RGD). The efficiency of the Michael addition reactions were determined by NMR and Ellman's assay. Successful decoupling of cell adhesivity and physical properties was demonstrated by quantifying and comparing the swelling ratios and Young's Moduli of various hydrogel formulations. Degradation profiles were established by incubating functionalized hydrogels in collagenase solutions (0.0 – 1.0 $\mu\text{g}/\text{mL}$), demonstrating that functionalized hydrogels degraded at a rate dependent upon collagenase concentration. Moreover, it was shown that the degradation rate was independent of CSP-RGD concentration. Cell attachment and proliferation on functionalized hydrogels were compared for various RGD concentrations, providing evidence that cell attachment and proliferation were directly related to relative amounts of the CSP-RGD combination peptide. An increase in cell viability was achieved using Michael addition techniques when compared to UV-polymerization, and was assessed by a LIVE/DEAD fluorescence assay. This photoinitiator-free method shows promise in creating hydrogel-based tissue engineering scaffolds allow for decoupled cell adhesivity and physical properties and that render greater cell viability.

© 2014 Elsevier Ltd. All rights reserved.

*Corresponding author: Tel.: +1-216-444-2484; Fax: +1-216-445-9535; MARCHAK@ccf.org.

Publisher's Disclaimer: This is a PDF file of an unedited manuscript that has been accepted for publication. As a service to our customers we are providing this early version of the manuscript. The manuscript will undergo copyediting, typesetting, and review of the resulting proof before it is published in its final citable form. Please note that during the production process errors may be discovered which could affect the content, and all legal disclaimers that apply to the journal pertain.

1. Introduction

The extracellular matrix (ECM) provides mechanical support and biochemical cues to ECM-adherent cells through a complex network composed of macromolecular proteins and polysaccharides [1–4]. Cell membrane-anchored integrins bind adhesive sequences present on proteins within the ECM microenvironment [2–5]. Anchorage dependent cells lose viability quickly when they are unable to bind to the supporting matrix [6]. Additionally, integrin binding stimulates signaling processes responsible for the production of interstitial collagenase, which aids in the degradation and remodeling of the microenvironment [1–4]. This remodeling is an important biological process needed for tissue regeneration, wound healing, and morphogenesis [2, 3]. Thus, the ECM serves as a mechanical scaffold for cells as well as a bioactive and dynamic environment that mediates cellular function [1–4]. Tissue engineering strategies have sought to mimic many of the supportive and biochemical properties of the ECM to guide the regeneration of specific tissues after loss of function induced by trauma or chronic disease [1, 7, 8].

The field of tissue engineering combines techniques from both engineering and life sciences to create artificial constructs to guide tissue repair and regeneration [3, 9]. Hydrogels provide a suitable platform for tissue engineered constructs due to their highly swollen three-dimensional environment similar to soft tissues, and a highly porous structure that permits transport of nutrients and cellular waste through the biomatrix [3, 4, 7, 9–11]. Biologically derived hydrogels have been developed from collagen and fibrin, which possess intrinsic biologically active components that mediate cell behavior [1, 3, 4, 12–14]. However, biologically derived hydrogels possess obvious drawbacks, including high batch-to-batch variability, the possibility of disease transmission, as well as non-selectivity [1, 3, 4, 7, 15]. To address these shortcomings, synthetic scaffold materials, such as poly(ethylene glycol) (PEG) hydrogels, have been employed for a wide range of applications including bone, cartilage, and blood vessel regeneration [1, 3, 9, 10, 16, 17]. PEG hydrogels have tunable mechanical properties that permit facile manipulation of the scaffold architecture and functionalized end groups [3, 7]. PEG hydrogels, however, are bioinert, resist protein adsorption, and do not support cell adhesion [3, 4, 9, 11, 18, 19]. In order to capitalize on the strengths of both biologically derived cell-interactive cues and tunability of synthetic hydrogels, extensive research has been performed in the conjugation of short bioactive peptides to synthetic materials to provide highly customizable bioactive hydrogels [3, 4, 8, 9, 14, 18, 19]. This approach provides the distinct advantage of quantitative control of cell-scaffold interactions while avoiding confounding results from ECM bound growth factors (commonly associated with biologically derived hydrogels), and resisting non-specific adsorption of exogenous proteins that can facilitate non-specific cell attachment to the material surface [3, 15]. Non-specific protein interactions with the biomaterial surface can have adverse effects such as inflammatory cell binding and foreign body responses [20, 21]. Copolymerizing synthetic bioactive peptide sequences derived from type I collagen such as GPQGIAGQ or the GRGDSP sequence from fibronectin have been utilized to promote enzyme-mediated degradation and cell adhesion to the hydrogel matrix, respectively [3, 4, 7, 14]. The peptide sequence derived from type I collagen has been shown to degrade in the presence of collagenase [3]. Combining these properties in a synthetic material allows for

the potential to design a wide range of temporary tissue engineered constructs that are degraded by collagenase from endogenous cells and gradually replaced with the body's own tissue over time.

Cell adhesive peptides linked to a PEG-diacrylate (PEGDA) network via PEG-monoacrylates (PEGMA) have been shown to be inefficient; and result in the formation of non-network terminal ends within the hydrogel matrix [3, 18]. The presence of these terminal ends results in a decrease in cross-link density, an inconsistency of the physical properties of the hydrogel network, and complicates comparisons between hydrogel formulations containing different RGD concentrations [14]. Moreover, polymerization techniques, such as UV-photopolymerization can adversely impact encapsulated cell viability due to prolonged exposure to cytotoxic free radicals or unreacted small molecules, as well as the photoinitiator compounds [10, 11, 22, 23]. To avoid these shortcomings, we investigated the copolymerization of a thiolated collagenase-sensitive peptide CGPQG↓IAGQC (CSP) (↓ indicating the cleavage site), a thiolated collagenase-sensitive and cell adhesive bi-functional peptide GPQG↓IAGQCGRGDSP (CSP-RGD), and four-arm PEG-acrylate using a mechanism known as Michael addition (Fig 1). The incorporation of cysteine in these sequences simultaneously served to introduce the enzymatically degradable sequence into the backbone of the otherwise bio-inert PEG hydrogel, and provides a means of crosslinking the network. The location of the middle cysteine in the bifunctional sequence allows for the cell adhesive RGD peptide to remain available for cell attachment. Under slightly basic conditions (pH 8.0), the nucleophilic thiols on the peptides react with the unsaturated acrylate groups on the four-arm PEG to form bioactive hydrogels with easily tunable parameters (cell-adhesivity and enzymatic biodegradability), physical properties independent of cell adhesive peptide concentration, and without UV-mediated photopolymerization. Hydrogels formed by Michael-type addition reactions are subject to a higher level of control since termination and radical transfer events are less relevant and there is no new polymeric species that is formed [8]. Moreover, hydrogels utilizing this technique can be formed under physiological conditions in direct contact with tissues, cells, and biological molecules and thus have utility as scaffolds for tissue engineering. These added benefits allow for the overall goal of designing a non-UV polymerized material that can incorporate both cell adhesive and biodegradable functionality independent of the physical properties. Such a material has the potential of being incorporated into a wide range of tissue-engineered constructs.

2. Materials and methods

2.1 Materials

All reagents were obtained from Sigma-Aldrich (St. Louis, MO) and used as received unless otherwise stated.

2.2 Instrumentation

Matrix-assisted laser desorption/ionization mass spectrometry (MALDI-MS) was performed on a Bruker Autoflex III (Billerica, MA) equipped with a standard linear detector and a gridless reflection detector. Samples were dissolved in 1:1 (v/v) ethanol and water and

mixed with the matrix solution of 2,5-dihydroxybenzoic acid before deposition on the stainless steel sample plate. Mass spectra were acquired from 500 laser shots. Parallel plate dynamic mechanical analysis was performed using a Perkin Elmer DMA7e (Waltham, MA). Phase contrast photomicrographs of cells were obtained on an inverted phase contrast microscope (Nikon Diaphot 200, Melville, NY) with a charge coupled display (CCD) camera using the Metamorph software package (version 6.2r6, Sunnyvale, CA).

2.3 Peptide Synthesis and Characterization

Thiol containing CSP and CSP-RGD were synthesized in a 1.0 mmol scale with Knorr resin with a loading of 0.89 mmol/g and 9-Fluoromethoxycarbonyl (Fmoc)-protected amino acids (Advanced Chem Tech, Louisville, KY) to produce an amide C-terminus on a solid phase peptide synthesizer (Applied Biosystems, Model 433A, Foster City, CA) using standard Fmoc chemistry. Peptides were cleaved from the resins and deprotected using trifluoroacetic acid (Fisher-Scientific, Pittsburgh, PA), precipitated in diethyl ether (Fisher-Scientific, Pittsburgh, PA), and dried in a vacuum oven. Peptides were purified by reverse-phase High Performance Liquid Chromatography (HPLC) on a 2690 Alliance system (Waters, Milford, MA), using a preparatory C18 column (XBridge, Model BEH130, Milford, MA) lyophilized, and stored at -20°C . Successful peptide synthesis was confirmed using MALDI-MS for molecular weight determination.

2.4 Cell Culture

Human Umbilical Vein Endothelial Cells (HUVECs, Lonza, Walkersville, MD), passages 4–7, were cultured with Endothelial Growth Media-2 (EGM-2, Lonza) containing 5% fetal bovine serum (FBS) and proprietary amounts of hydrocortisone, basic human fibroblast growth factor, vascular endothelial growth factor (VEGF), insulin-like growth factor, ascorbic acid, and human recombinant epidermal growth factor. All cell culture was performed at 37°C , 5% CO_2 , grown to 80–90% confluence, and subsequently passaged in EGM-2. All materials used for cell culture were received sterile or were steam sterilized prior to use unless otherwise noted.

2.5 3D Hydrogel Preparation and Characterization

Michael addition functionalized hydrogels were formed by filtering peptide and four-arm PEG acrylate (Layson Bio, Huntsville, AL) solutions separately using a $0.2\ \mu\text{m}$ nylon syringe filter, and mixing in a 2:1 molar ratio, to allow stoichiometric equivalents of thiol and acrylate functional groups in 0.1 M sodium phosphate solution containing 1 mM ethylenediaminetetraacetic acid (EDTA) (pH 8.0). For swelling ratio characterization and degradation $60\ \mu\text{L}$ of hydrogel precursor solutions of 5% or 10% w/v were dispensed into a teflon mold for 10 minutes. For dynamic mechanical analysis (DMA) testing, $100\ \mu\text{L}$ of 10% w/v hydrogel precursor solution was dispensed into a 11 mm diameter mold for 10 minutes. For cell attachment and proliferation studies, 18 mm glass coverslips were cleaned by sonication in chloroform followed by 15 min treatment by radio frequency (RF) glow discharge from argon bubbled through water. The coverslips were then coated with γ -methacryloxypropyl trimethoxysilane in 95% ethanol and 5% DI (v/v) solution adjusted to pH 5 with glacial acetic acid for 2 hours, rinsed with excess ethanol, and dried in vacuo in covered glass petri dishes at 110°C to sterilize the silanized coverslips. Poly(ethylene

terephthalate) (PET) sheets (McMaster-Carr, Cleveland, OH) were cleaned by subsequent sonication in DI and then in ethanol, treated by RF glow discharge, and sterilized with ethylene oxide. Hydrogel precursor solution (5% w/v) was quickly pipetted onto PET sheets, covered with silanized glass coverslips, and polymerized for 10 minutes at room temperature. The assembly was inverted and submerged in phosphate buffered saline (PBS) (GIBCO, Grand Island, NY). The PET sheet was peeled away leaving a thin hydrogel film bound to the glass coverslip.

2.6 Reaction Efficiency

To quantify Michael addition reaction efficiency, disappearance of the terminal thiols on the peptides was measured by Ellman assay (Thermo Scientific Pierce, Rockford, IL). The Ellman's reagent (5,5'-dithio-bis-[2-nitrobenzoic acid]) reacts with sulfhydryl groups to yield a colored product, allowing for the quantification of cysteines in solution. To assess disappearance of the thiol functional group, four-arm PEG acrylate (Layson Bio, Huntsville, AL) was combined with CSP or CSP-RGD in a 2:1 molar ratio in 0.1 M sodium phosphate solution containing 1 mM EDTA (pH 8.0), allowing for a 3-fold excess of acrylate to thiol functional groups to ensure reagents did not polymerize. Thiol concentration was measured both prior to the Michael addition reaction, and 10 minutes after the reaction occurred by measuring absorbance at a wavelength of 412 nm on a Biotek Synergy H1 Hybrid Reader (Winooski, VT). Reaction efficiency was calculated by comparing the absorbance values for pre-reaction and post-reaction thiol concentrations (Eqs 1 & 2).

In addition, reaction efficiency was measured by quantifying disappearance of the acrylate from PEG by combining multi-arm PEG acrylate with CSP or CSP-RGD in a 2:1 molar ratio, to avoid polymerization, 0.1 M sodium phosphate solution containing 1 mM EDTA (pH 8.0) for 10 minutes. The solution was then dialyzed (500 Da MWCO, Spectrum Laboratories, Rancho Dominguez, CA) for 6 hours, replacing DI water every 2 hours, to remove salts. The sample was then frozen at -80°C for 24 hours, and lyophilized for 24 hours. The lyophilized product was dissolved in CDCl_3 and ^1H NMR was taken. The degree of PEG acrylation post-reaction was quantified by comparing the three hydrogen peaks associated with the acrylate functional group on PEG with the hydrogen peaks associated with the PEG repeat unit (Eq 3). The theoretical acrylation post-reaction was calculated using the stoichiometric ratio of functional groups (Eq 4). The reaction efficiency was obtained by comparing the actual and theoretical post-reaction acrylation values (Eq 5).

$$A_{Theoretical} = A_{Cysteine} \left(1 - \frac{\#acrylates}{\#thiols}\right) \quad (1)$$

$$Reaction\ Efficiency = 100 - \left[\frac{(A_{Actual} - A_{Theoretical})}{A_{Theoretical}} * 100 \right] \quad (2)$$

$$Acrylation_{Actual} = \frac{(Acrylate\ H\ peaks) * (MW\ of\ PEG) * (\#H\ per\ PEG\ repeat\ unit)}{(\#acrylate\ H\ per\ PEG) * (repeat\ unit\ H\ peak) * (MW\ PEG\ repeat\ unit)} \quad (3)$$

$$Acrylation_{Theoretical} = (Acrylation_{PEG}) \left(1 - \frac{\#thiols}{\#acrylates}\right) \quad (4)$$

$$Reaction\ Efficiency = 100 - \left[\frac{(Acrylation_{Actual} - Acrylation_{Theoretical})}{Acrylation_{Theoretical}} * 100 \right] \quad (5)$$

2.7 Hydrogel Swelling Ratio

Four-arm PEG hydrogels (10% w/v) with cell adhesive peptide concentrations of 0 mM, 1.4 mM, 2.9 mM, and 4.3 mM (or CSP-RGD to CSP and RGD to CSP molar ratios of 0:7, 1:6, 2:5, and 3:4 respectively) were synthesized in triplicate as previously described in section 2.5, and incubated in excess DI overnight to allow them to swell. In these studies, CSP-RGD represents the inclusion of the bifunctional peptide whereby the cell adhesive sequence is incorporated into the backbone of the hydrogel network, and RGD refers to the cell adhesive sequence attached terminally to the multi-arm PEG. For comparison, four-arm PEG hydrogels (5% w/v) with CSP as the crosslinker, UV polymerized PEG hydrogels (5% w/v), and Matrigel (BD biosciences, San Jose, CA) were also synthesized as described in section 2.5 and swollen overnight. The swollen hydrogels had excess fluid removed by weigh paper and were weighed to obtain the wet weight of the swollen hydrogel (W_{wet}). The swollen hydrogel disks were freeze-dried to obtain the dry weight of the hydrogel (W_{dry}). The Swelling Ratio (Q_m) of hydrogels was calculated (Eq. 6):

$$Q_m = \frac{W_{wet} - W_{dry}}{W_{dry}} * 100\% \quad (6)$$

2.8 Hydrogel Stiffness

Four-arm PEG hydrogels (10% w/v) with cell adhesive peptide concentrations of 0 mM, 1.4 mM, 2.9 mM, and 4.3 mM, were synthesized in triplicate as previously described in section 2.5 and incubated in excess DI overnight to allow them to swell. The swollen hydrogels were placed between two parallel plates on a dynamic mechanical analyzer, and probe displacement was quantified as a function of static force during compression of the hydrogels. The static force applied to the hydrogels ranged from 0 to 10 mN, and the linear portion of the dataset was determined and used to calculate the Young's Modulus for each of the samples.

2.9 Hydrogel Degradation

To test the enzyme mediated degradation of the CSP peptide modified PEG hydrogels, 10% (w/v) hydrogels were synthesized as previously described in section 2.5. Hydrogels were swollen in Hank's Balanced Salt Solution (HBSS) purchased from GIBCO (Grand Island, NY) for 24 hours at room temperature to allow for equilibration, and the wet weight was taken to establish a weight at time 0. HBSS was replaced with 0, 0.125, 0.25, 0.5, 1.0 $\mu\text{g/mL}$ collagenase obtained from Clostridium histolyticum in HBSS solution and incubated at 37°C. Separately, CSP-RGD PEG hydrogels (10% w/v) were synthesized as previously

described in section 2.5, to test the effect of the RGD sequence on degradation rate. The same procedure was followed in swelling these hydrogels, and the HBSS was replaced with 0.125 µg/mL collagenase solution. Hydrogels were weighed at two hour time points until the mass of the hydrogel decreased to less than 50% of the original mass, and were subsequently weighed every hour until they had completely degraded. The collagenase solution was changed every hour until the hydrogels degraded. The percent wet weight was then calculated by dividing by the hydrogel weight by the weight at time 0.

2.10 Cell Attachment & Proliferation

Four-arm PEG hydrogels (5% w/v) were synthesized on coverslips as described in section 2.5. A fibronectin (FN) surface was prepared and served as the positive control. Fibronectin is often used as a positive control in cell attachment studies, due to the cell adhesive RGD sequence found in this protein. The fibronectin surface was prepared by incubating FN isolated from human plasma in PBS at a density of 1 µg/cm² at 37°C for 2 hours on the bottom of a coated tissue culture polystyrene plate. The PBS was removed immediately before cell seeding. A 1.0 mL HUVEC suspension in serum and growth factor free Endothelial Basal Media-2 (EBM-2) containing no growth factors, cytokines, or supplements with seeding density of 1.5×10^4 cells/cm² was incubated at 37 °C at 5% CO₂ for 6 hours on top of the functionalized hydrogels. EBM-2 was then exchanged for Endothelial Growth Media-2 (EGM-2), and media was changed every 2 days. The serum-free conditions used during cell seeding ensured that all cell adhesion was due to the presence of the RGD peptide rather than from exogenous serum proteins that would otherwise contribute to nonspecific binding. Cells were imaged using inverted phase contrast microscopy at 1, 4, and 7 days. Cell density was indirectly assessed by measuring DNA concentration using Picogreen assay (Invitrogen, Carlsbad, CA). At 1, 4, and 7 day time points media was removed from functionalized hydrogels and FN surfaces seeded with HUVECs. The hydrogels and FN surfaces were rinsed twice with PBS and frozen overnight to arrest cell growth. Hydrogels were then incubated with Quant-iT Picogreen dsDNA reagent (Invitrogen, Carlsbad, CA) in 20× CyQUANT lysis buffer (Invitrogen, Carlsbad, CA) following manufacturer's instructions. 100 µL samples were transferred to a 96 well plate and fluorescence produced by the Picogreen reagent binding to the dsDNA was measured using a Biotek Synergy H1 Hybrid Reader at a 260 nm wavelength. Fluorescence was then correlated to a standard curve using known concentrations of calf thymus DNA (Invitrogen, Carlsbad, CA) to assess DNA concentration.

2.11 Cell Encapsulation Viability

To quantify acute toxicity, cell encapsulated 3D sandwich hydrogels (5% w/v) were synthesized by Michael addition and UV polymerization. Michael addition functionalized hydrogel precursor solution was prepared by filtering peptide and four-arm PEG acrylate solutions separately using a 0.2 µm nylon syringe filter, and mixing in a 2:1 molar ratio, to allow stoichiometric equivalents of thiol and acrylate functional groups in 0.1 M sodium phosphate solution containing 1 mM ethylenediaminetetraacetic acid (EDTA) (pH 8.0). Since equal volume fractions of peptide and PEG solutions were combined, the resultant solution was a 5% w/v PEG solution with stoichiometrically equivalent proportions of acrylate and thiol functional groups. By contrast, UV polymerized functionalized hydrogel

precursor solution (5% w/v) was prepared by filtering a solution of acrylate-PEG-CSP-PEG-acrylate with 0.1 % (w/v) irgacure 2959 (1-[4-[2-Hydroxyethoxy]-phenyl]-2-hydroxy-2-methyl-1-propane-1-one) (Ciba Specialty Chemicals, Tarrytown, NY) dissolved in EDTA through a 0.2 μm nylon syringe filter. 20 μL of each hydrogel precursor solution was dispensed into a teflon mold and polymerized for 10 minutes. Only UV polymerized hydrogels were placed under a 365 nm wavelength UV-lamp during this time. An additional 20 μL hydrogel precursor solution containing 250 HUVECs/ μL was pipetted on top of the first layer and polymerized for 10 minutes as before. A final layer of HUVEC-free hydrogel precursor solution was then pipetted on top of the second layer and polymerized for an additional 10 minutes as before. The resultant hydrogels were comprised of a HUVEC containing layer between two HUVEC free hydrogel layers. To visualize live vs. dead cells for each synthesis method a LIVE/DEAD assay (Invitrogen, Carlsbad, CA) was performed. A working solution of 4 μM calcein AM and 4 μM ethidium-1 homodimer (EthD-1) was made in PBS, to stain living cells and dead cells respectively. One mL of the working solution was dispensed on the cell encapsulated hydrogels and then incubated for 30 minutes at 37° C. Overlapping images were taken with an inverted epifluorescent microscope containing a dual fluorescein isothiocyanate (FITC) and Texas Red filter system. To assess the degree of living versus dead cells, cells were counted that were stained with calcein AM (green) and EthD-1 (red) for UV-polymerized and Michael-addition synthesized hydrogels. A live cell percentage was then calculated (Eq. 7)

$$\text{Percent Live Cells} = 100 \times \frac{HUVEC_{LIVE}}{(HUVEC_{LIVE} + HUVEC_{DEAD})} \quad (7)$$

2.12 Statistics

Data are represented as mean \pm standard deviation of at least 3 samples. Statistical analysis was performed using student's t-tests for single comparisons. A p value < 0.05 was considered significant.

3. Results

3.1 Characterization of bioactive peptides

MALDI spectra of CSP, RGD, and CSP-RGD confirmed the molecular weight of the synthesized peptides (Fig. 2). Peaks at 954.11 and 969.91 represent successful synthesis of the collagenase sensitive peptide, peaks at 689.86, 711.83, and 727.82 correspond to the cell adhesive peptide, and peaks at 1500.88 and 1522.87 correspond to successful synthesis of the collagenase sensitive and cell adhesive combination peptide.

3.2 Peptide Reaction Efficiency

The ^1H NMR of 4-arm PEG acrylate in CDCl_3 showed a baseline acrylation percent of 91.5%. After reacting 4-arm acrylate with CSP in a PEG:CSP ratio of 2:1, the acrylation percent dropped to 71.13 suggesting a 99.5% reaction efficiency. After reacting 4-arm PEG acrylate with CSP-RGD in a PEG:CSP-RGD ratio of 2:1, the acrylation percent dropped to 72.7% suggesting a reaction efficiency of 94.1%. Results were corroborated using the

Ellman's assay which showed a 98.1% and 95.2% reaction efficiency for the CSP & CSP-RGD peptides respectively.

3.3 Hydrogel Preparation and Characterization

Four-arm PEG hydrogels (10% w/v) synthesized with CSP-RGD concentrations of 0 mM, 1.4 mM, 2.9 mM, and 4.3 mM had swelling ratios of 27.8 ± 1.6 , 26.9 ± 1.6 , 27.1 ± 1.5 , and 27.6 ± 1.1 respectively, resulting in no statistical difference in swelling ratio (Q_m). Under the same processing conditions four-arm PEG hydrogels (10% w/v) with RGD concentrations of 0 mM, 1.4 mM, 2.9 mM, and 4.3 mM had swelling ratios of 27.8 ± 1.6 , 46.9 ± 1.8 , 76.9 ± 13.8 , and no formed hydrogel respectively. The results demonstrate that the physical properties of the hydrogels do not significantly differ with respect to the CSP-RGD concentration suggesting that incorporating the RGD into the backbone of the hydrogel network preserves its structural integrity. Conversely, when the RGD peptide was not incorporated into the backbone, the terminal ends formed greatly increased the swelling ratio due to the decreased cross link density (Fig 3A). The effect of terminal ends on hydrogel swelling ratio and crosslink density has been previously assessed using monoacrylated PEG and corroborates our results with regards to the inclusion of terminally conjugated peptides [18].

Four-arm PEG hydrogels (10% w/v) synthesized with CSP-RGD concentrations of 0 mM, 1.4 mM, 2.9 mM, and 3.4 mM possessed Young's Moduli of 5.0 ± 0.5 , 4.3 ± 0.3 , 4.7 ± 0.5 , and 4.5 ± 0.2 kPa respectively. Four-arm PEG hydrogels (10% w/v) synthesized with these same concentrations of the RGD peptide possessed Young's Moduli of 5.0 ± 0.5 , 1.2 ± 0.3 , 0.08 ± 0.02 kPa respectively. These results corroborate the swelling ratio data, further indicating that the backbone linked RGD concentration does not significantly affect the physical properties of the hydrogel, whereas terminally linked RGD does have a significant effect on the physical properties (Fig 3B).

Four-arm PEG hydrogels (5% w/v) both synthesized using Michael addition and UV polymerization had considerably higher swelling ratios of 53.0 ± 2.0 and 54.7 ± 2.2 respectively. These results demonstrate that 5% (w/v) hydrogels had a swelling ratio that more closely resembled that of Matrigel (57.8 ± 3.1), which often used as a gold standard in cell studies. Thus, these hydrogels were deemed more appropriate for use in our cell attachment and cell survival studies (Fig 4).

3.4 Collagenase-Mediated Hydrogel Degradation

In the absence of collagenase (0 $\mu\text{g}/\text{mL}$ collagenase in HBSS) CSP-PEG hydrogels showed no degradation, as indicated by no significant mass change at 11 hours. In the presence of collagenase, the CSP-PEG hydrogels degraded at a rate dependent upon collagenase concentration. In the case of 0.125 $\mu\text{g}/\text{mL}$ collagenase concentration, the hydrogels gained mass during early time points. This is attributed to a decrease in crosslinking density with increased water swelling of the hydrogels. When the degradation passes a critical time point, the cross-link density becomes too low to maintain the hydrogel network and hold the water. As a result, the hydrogel network collapses and fully degrades. The graph shows that hydrogels degraded in 11 hours when incubated in 0.125 $\mu\text{g}/\text{mL}$ collagenase, 8 hours in 0.25

$\mu\text{g/mL}$, 5 hours in $0.5 \mu\text{g/mL}$, and 4 hours in $1.0 \mu\text{g/mL}$ (Fig 5A). Hydrogels with CSP-RGD concentrations of 0 mM, 1.4 mM, 2.9 mM, and 4.3 mM had similar enzyme-mediated degradation profiles, with no statistically significant deviation, and all hydrogels completely degraded within 11 hours. This suggests that the presence of backbone linked RGD peptide has no observable effect on the degradation rates of the hydrogels (Fig 5B).

3.5 Endothelial Cell Attachment and Proliferation on Functionalized Hydrogels

At day 1, the negative control surface, which contained no CSP-RGD bifunctional peptide, had minimal cell attachment, whereas the fibronectin surface serving as the positive control had the most number of adherent cells. At this time point, there was a direct correlation between endothelial cell attachment and CSP-RGD concentration was observed, with minimal cell attachment on the negative control surface without CSP-RGD. At day 4, all surfaces showed an increase in cell population with the exception of the negative control. The FN surface had achieved confluence by this time point. At day 7, all surfaces showed an increase in cell population with the exception of the negative control surface. The FN positive control surface displayed a decrease in cell number, possibly due to detachment of cells caused by over-confluence. The cell growth was directly dependent upon the concentration relative ratio of CSP-RGD : CSP, with only the 4.3 mM surface and fibronectin surface reaching confluence by day 7 (Fig. 6).

3.6 Endothelial Cell Survival for Michael Addition vs. UV Polymerized Hydrogels

Acute cell toxicity was assessed by counting both live and dead cells, and using Eq. 7 to express percent live cells after polymerization. Percent live endothelial cell values encapsulated using the Michael addition and UV-polymerization were 80.9 ± 9.2 , and 52.1 ± 9.1 respectively. This difference in endothelial cell survival can be attributed to the absence of photoinitiator and lack of UV exposure in the Michael addition hydrogels (Fig. 7).

4. Discussion

In order for anchorage-dependent cells to function appropriately *in vitro*, they must sustain contacts with neighboring cells and/or the ECM [2, 6]. The ECM imparts cell signaling through various cell surface growth factor receptors and adhesion molecules such as integrins [2–5]. ECM proteins can determine cell behavior, migration, differentiation, proliferation and survival by communicating with the intracellular cytoskeleton and transmission of growth factor signals [1–4, 9]. Previous research has focused on incorporating biologically active peptide sequences into hydrogels in order to synthesize materials that mimic the ECM [1, 3, 4, 7–9]. Many approaches utilize non-backbone linked cell adhesive peptides which affect the physical properties of the hydrogel matrix, or rely on cytotoxic UV-polymerization techniques [3, 10, 11]. Additionally, studies have examined the survival rate of cells and changes in cell behavior in response to the incorporation of photoinitiators into hydrogel formulations [11, 23]. In these studies, survival rates ranged from approximately 53% to 88% depending on which photoinitiator was used, making evident the need for more appropriate polymerization techniques that do not include cytotoxic agents [11]. By contrast, studies have demonstrated that Michael addition techniques can successfully encapsulate cells with survival rates up to 95% [10]. Our study

revealed an average live cell percent of $80.9\% \pm 9.2$ for Michael addition techniques. This slightly lower value may be attributed to the processing time it took to synthesize the sandwich hydrogels, in which the cells were incubated in hydrogel precursor solution rather than media for a total of 20 minutes. This live cell percentage is still significantly higher than the percent living cells in hydrogels polymerized using UV ($52.1\% \pm 9.1$), however. The sandwich method was employed to ensure that the cells were completely encapsulated in the hydrogel network, as to better mimic a three-dimensional tissue engineered construct in which this material would be designed for.

Decoupling the cell adhesive properties from the physico-mechanical properties of the hydrogel allows for more control over the scaffold material, and for more accurate comparisons between hydrogel formulations. A material that uses thiolated bifunctional cell adhesive and enzyme degradable peptide sequences in conjunction with multi-arm PEG acrylate, can address both of these issues simultaneously.

^1H NMR and Ellman's assay measured high reaction efficiency for both CSP and CSP-RGD. This suggests that there is no observable decrease in thiol reactivity toward PEG acrylate when the cysteine is incorporated into the middle of the peptide when compared to a terminal cysteine. Bioactive hydrogels containing various ratios of the bifunctional CSP-RGD peptide possessed no significant difference in either the swelling ratios or Young's Moduli. This uniformity in the swelling ratio and Young's Modulus suggests a relative consistency in the physical properties of the hydrogels using the bifunctional peptide, and indicates an effective decoupling of the cell adhesive properties from the cross-link density. The hydrogels synthesized using various ratios of the non-backbone linked RGD peptide had significant differences in cross-link density and Young's Moduli, by contrast, suggesting that the physical properties of the hydrogel were a function of terminally linked cell adhesive peptide concentration. Previous studies have demonstrated that the presence of non-backbone linked terminal ends have a significant effect on network properties, and cause a measurable difference in hydrogel properties such as swelling ratio and shear modulus in hydrogels with low cross-linking densities [18]. Whereas studies utilized polyethylene glycol monoacrylate to form terminal ends, a similar pattern was observed with the inclusion of non-backbone linked RGD peptides.

Endothelial cells rely on integrin binding sites such as the fibronectin derived GRGDSP sequence to attach and proliferate [24]. We have demonstrated that the Michael addition synthesis technique successfully produces bioactive hydrogel networks that allow for endothelial cell adhesion and proliferation as a function the cell adhesive peptide when incorporated into the backbone of the hydrogel. Endothelial cells seeded on sufficiently high relative amounts of the cell adhesive peptide (4.3 mM CSP-RGD or 3:4 CSP-RGD:CSP) result in similar binding and proliferation as native fibronectin. This is indicative of achieving biomimetic cell-adhesiveness in our synthetic scaffolds. On two-dimensional surfaces, it has been established that ligand densities of 6×10^5 ligands/mm² are optimal for endothelial cell binding [5]. Our studies demonstrate that while lower ligand densities (a theoretical value of approximately 1.8×10^5 ligands/mm² for the 3:4 experimental surface) may not present as many endothelial cell binding sites as fibronectin, within the course of 7

days, these surfaces can achieve endothelial cell densities comparable to a fibronectin surface.

5. Conclusion

ECM-mimetic hydrogels can be synthesized by conjugating bioactive peptide sequences to an otherwise bioinert PEG backbone. Though previous synthesis techniques have relied on incorporating cell adhesive peptides by the formation of non-backbone terminal ends, or the incorporation of cytotoxic free-radicals, the reported technique of combining bi-functional peptide sequences and four-arm PEG acrylate using Michael addition, eliminates these shortcomings. Taken together this photoinitiator-free technique of synthesizing peptide-modified hydrogels successfully produces scaffold materials that are enzymatically degradable and capable of supporting cell adhesion and proliferation, while allowing control over the hydrogel properties and eliminating the need for UV-polymerization.

ACKNOWLEDGEMENTS

The project described was supported by Grant Number 5RC1EB010795 and Grant Number 1R01HL087843 for the National Heart, Lung, and Blood Institute. The content is solely the responsibility of the authors and does not necessarily represent the official views of the National Institutes of Health.

REFERENCES

1. Hubbell JA. Materials as morphogenetic guides in tissue engineering. *Curr Opin Biotechnol.* 2003; 14(5):551–558. [PubMed: 14580588]
2. Kim SH, Turnbull J, Guimond S. Extracellular matrix and cell signalling: the dynamic cooperation of integrin, proteoglycan and growth factor receptor. *J Endocrinol.* 2011; 209(2):139–151. [PubMed: 21307119]
3. Zhu J. Bioactive modification of poly(ethylene glycol) hydrogels for tissue engineering. *Biomaterials.* 2010; 31(17):4639–4656. [PubMed: 20303169]
4. Zhu J, Marchant RE. Design properties of hydrogel tissue-engineering scaffolds. *Expert Rev Med Devices.* 2011; 8(5):607–626. [PubMed: 22026626]
5. Le Saux G, et al. The relative importance of topography and RGD ligand density for endothelial cell adhesion. *PLoS One.* 2011; 6(7):e21869. [PubMed: 21779342]
6. Re F, et al. Inhibition of anchorage-dependent cell spreading triggers apoptosis in cultured human endothelial cells. *J Cell Biol.* 1994; 127(2):537–546. [PubMed: 7523422]
7. Wang X, et al. Hyaluronic acid-based scaffold for central neural tissue engineering. *Interface Focus.* 2012; 2(3):278–291. [PubMed: 23741606]
8. Kloxin AM, et al. Mechanical properties of cellularly responsive hydrogels and their experimental determination. *Adv Mater.* 2010; 22(31):3484–3494. [PubMed: 20473984]
9. Hou Y, et al. Photo-cross-linked PDMSstar-PEG hydrogels: synthesis, characterization, and potential application for tissue engineering scaffolds. *Biomacromolecules.* 2010; 11(3):648–656. [PubMed: 20146518]
10. Jin R, et al. Synthesis and characterization of hyaluronic acid-poly(ethylene glycol) hydrogels via Michael addition: An injectable biomaterial for cartilage repair. *Acta Biomater.* 2010; 6(6):1968–1977. [PubMed: 20025999]
11. Mironi-Harpaz I, et al. Photopolymerization of cell-encapsulating hydrogels: crosslinking efficiency versus cytotoxicity. *Acta Biomater.* 2012; 8(5):1838–1848. [PubMed: 22285429]
12. Koga M, et al. Contribution of rat endothelial progenitor cells on three-dimensional network formation in vitro. *Tissue Eng Part A.* 2009; 15(9):2727–2739. [PubMed: 19226220]
13. Takayama T, et al. The growth of a vascular network inside a collagen-citric acid derivative hydrogel in rats. *Biomaterials.* 2009; 30(21):3580–3587. [PubMed: 19362365]

14. Zusiak SP, Durbal R, Leach JB. Influence of cell-adhesive peptide ligands on poly(ethylene glycol) hydrogel physical, mechanical and transport properties. *Acta Biomater.* 2010; 6(9):3404–3414. [PubMed: 20385260]
15. Cushing MC, Anseth KS. Materials science. Hydrogel cell cultures. *Science.* 2007; 316(5828): 1133–1134. [PubMed: 17525324]
16. Watkins AW, Anseth KS. Copolymerization of photocrosslinkable anhydride monomers for use as a biodegradable bone cement. *J Biomater Sci Polym Ed.* 2003; 14(3):267–278. [PubMed: 12713099]
17. Burdick JA, Anseth KS. Photoencapsulation of osteoblasts in injectable RGD-modified PEG hydrogels for bone tissue engineering. *Biomaterials.* 2002; 23(22):4315–4323. [PubMed: 12219821]
18. Beamish JA, et al. The effects of monoacrylated poly(ethylene glycol) on the properties of poly(ethylene glycol) diacrylate hydrogels used for tissue engineering. *J Biomed Mater Res A.* 2010; 92(2):441–450. [PubMed: 19191313]
19. Hern DL, Hubbell JA. Incorporation of adhesion peptides into nonadhesive hydrogels useful for tissue resurfacing. *J Biomed Mater Res.* 1998; 39(2):266–276. [PubMed: 9457557]
20. Bridges AW, Garcia AJ. Anti-inflammatory polymeric coatings for implantable biomaterials and devices. *J Diabetes Sci Technol.* 2008; 2(6):984–994. [PubMed: 19885288]
21. Anderson JM, Rodriguez A, Chang DT. Foreign body reaction to biomaterials. *Semin Immunol.* 2008; 20(2):86–100. [PubMed: 18162407]
22. Fedorovich NE, et al. The effect of photopolymerization on stem cells embedded in hydrogels. *Biomaterials.* 2009; 30(3):344–353. [PubMed: 18930540]
23. Rouillard AD, et al. Methods for photocrosslinking alginate hydrogel scaffolds with high cell viability. *Tissue Eng Part C Methods.* 17(2):173–179. [PubMed: 20704471]
24. Joshi P, et al. Endothelial cells adhere to the RGD domain and the fibrinogen-like terminal knob of tenascin. *J Cell Sci.* 1993; 106(Pt 1):389–400. [PubMed: 7505785]

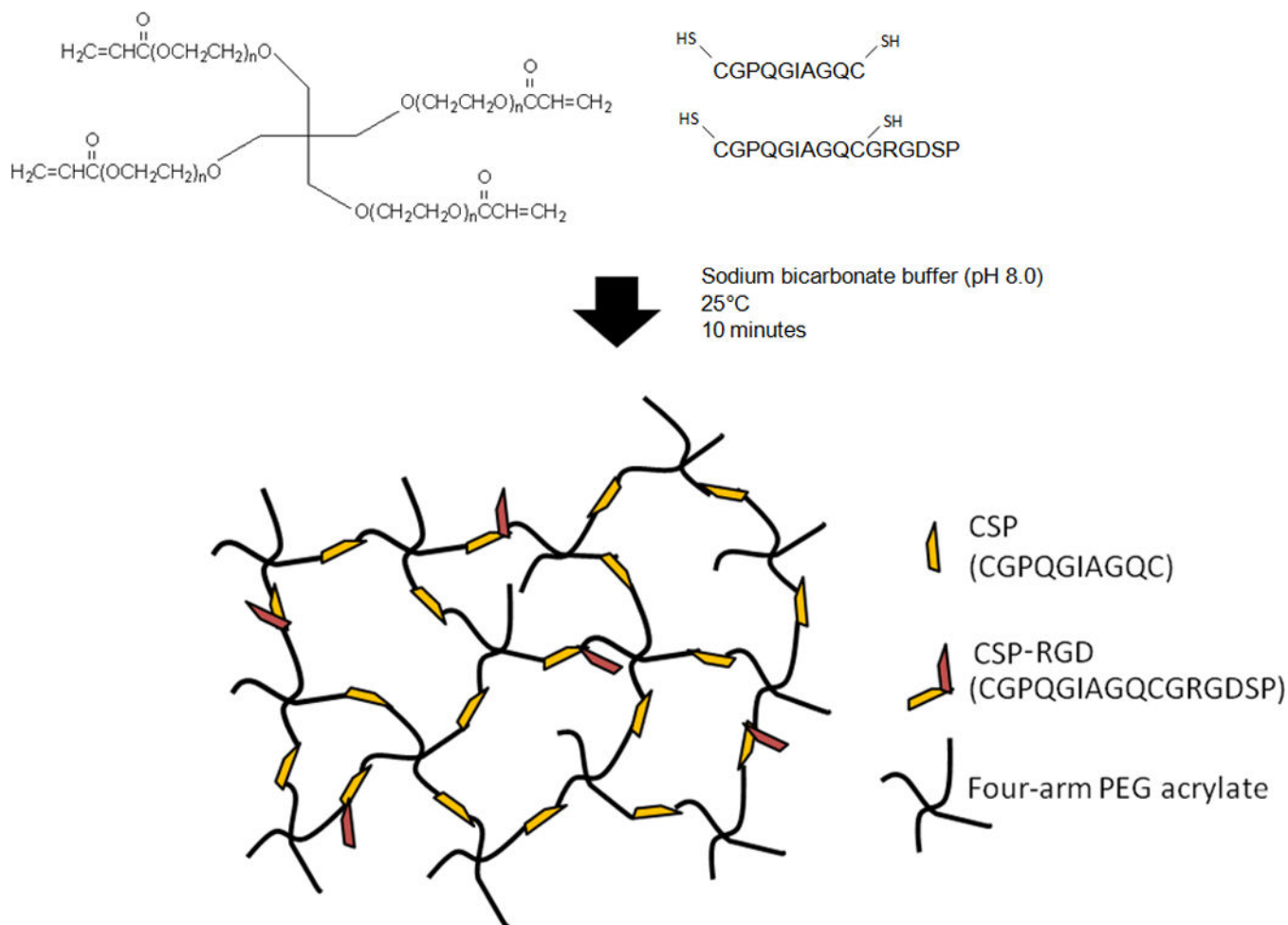


Figure 1. Bio-active 4-arm PEG hydrogels containing CSP and CSP-RGD allows for simultaneous cell attachment and enzymatic degradation. Combining 4-arm PEG acrylate with cysteine containing peptides at pH 8.0 allows for stoichiometric equivalence of the acrylate and thiol functional groups, and the incorporation of the collagenase sensitive peptide and the RGD peptide in the backbone of the hydrogel network.

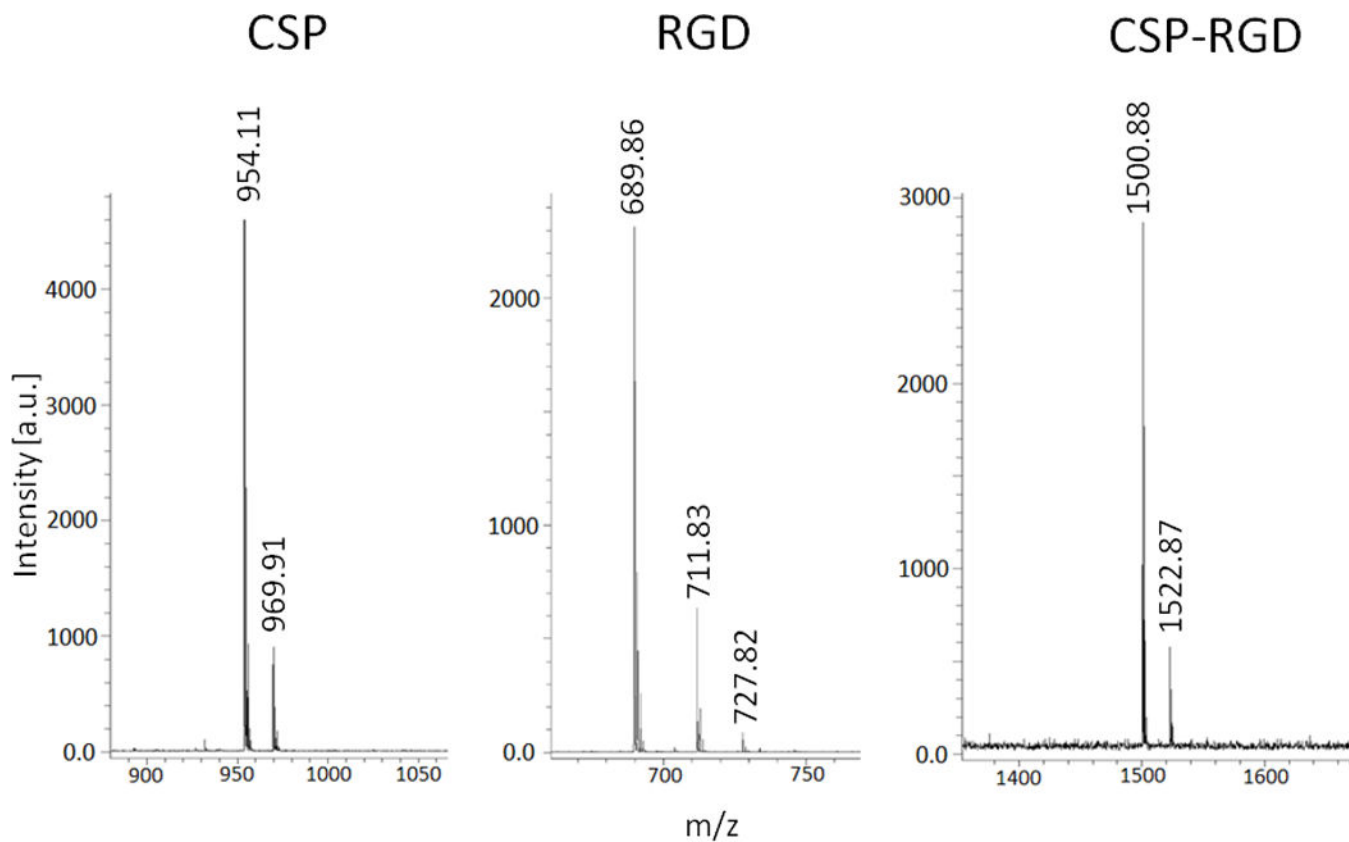


Figure 2.

Mass spectroscopy peaks of molecular weights of 954.11 and 969.91 correspond to CGPQGIAGQC (left), peaks at 689.86, 711.83, and 727.82 correspond to CGRGDSP (middle), and peaks of molecular weight 1522.87 and 1500.88 correspond to the combination sequence CGPQGIAGQCGRGDSP (right). Multiple peaks in the spectra are due to the association with sodium and potassium ions.

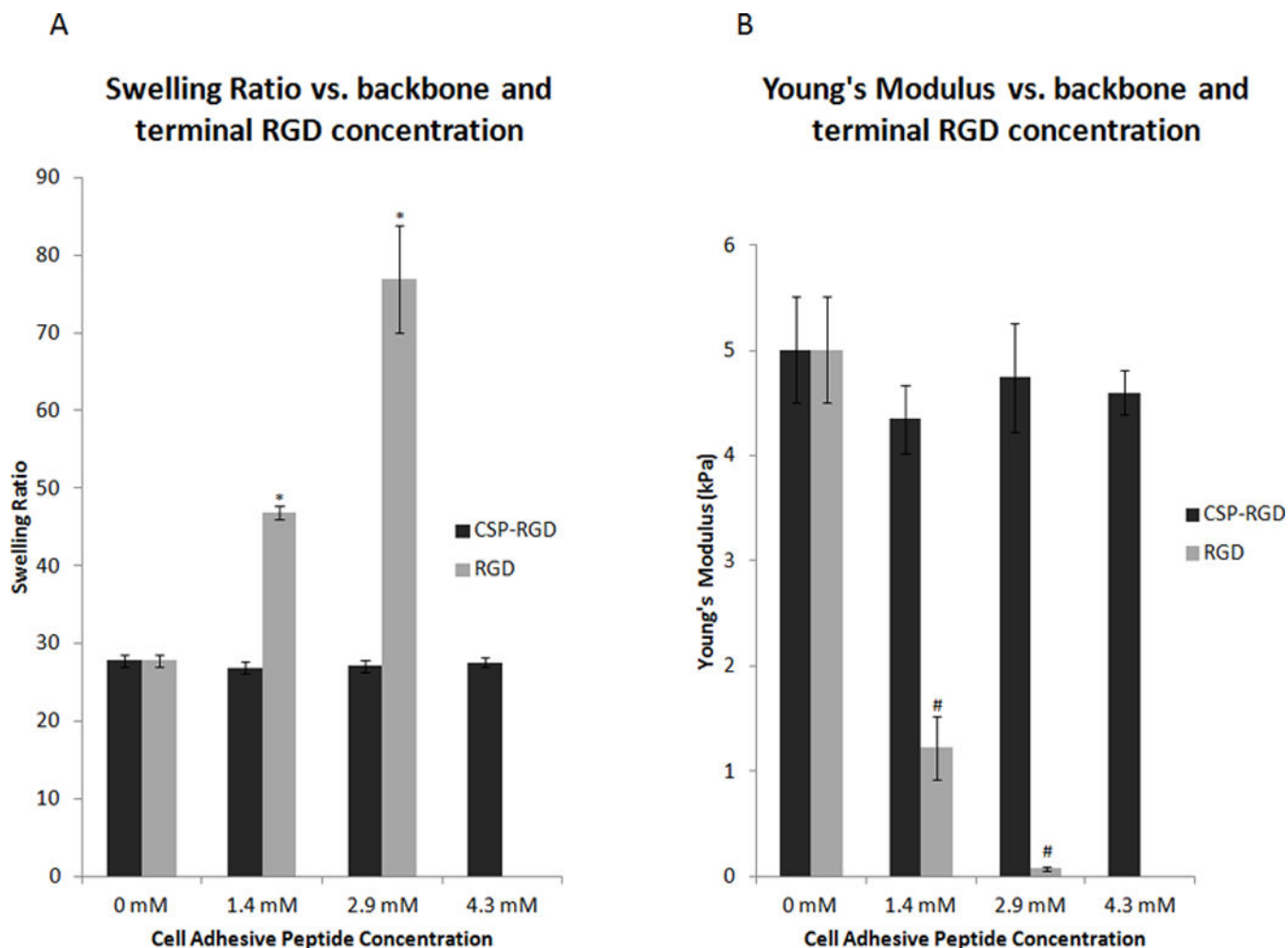


Figure 3.

(A) Average swelling ratios for four-arm PEG hydrogels (10% w/v) with CSP-RGD (black bars) and RGD (grey bars) peptide concentrations of 0 mM, 1.4 mM, 2.9 mM, and 4.3 mM. CSP-RGD represents hydrogels where the cell adhesive peptide was attached to the backbone of the polymer network, whereby RGD refers to hydrogels that had the cell adhesive peptide attached to terminal ends of PEG. Hydrogels containing the combination CSP-RGD sequence displayed no significant change in swelling ratio with respect to concentration of the combination peptide. Hydrogels containing the RGD sequence possessed significant increases in swelling ratio with respect to the RGD peptide concentration. *: $p < 0.05$ compared to CSP-RGD hydrogels with the same cell adhesive peptide concentration. (B) Young's Modulus for four-arm PEG hydrogels (10% w/v) with CSP-RGD concentrations of 0 mM, 1.4 mM, 2.9 mM, and 4.3 mM were 5.0 ± 0.5 , 4.3 ± 0.3 , 4.7 ± 0.5 , and 4.6 ± 0.2 kPa respectively. Young's Modulus for four-arm PEG hydrogels (10% w/v) with these same concentrations of RGD peptide were 5.0 ± 0.5 , 1.2 ± 0.3 , 0.1 ± 0.02 and no hydrogel formed respectively. The force applied to the hydrogels ranged from 8 mN to 10 mN. There was no significant difference in the Young's Modulus of any of the hydrogel samples when the RGD sequence was linked to the backbone of the hydrogel network, however, terminally linked RGD resulted in a significant change in Young's

Modulus, #: $p < 0.05$ compared to CSP-RGD hydrogels with the same cell adhesive peptide concentration.

Author Manuscript

Author Manuscript

Author Manuscript

Author Manuscript

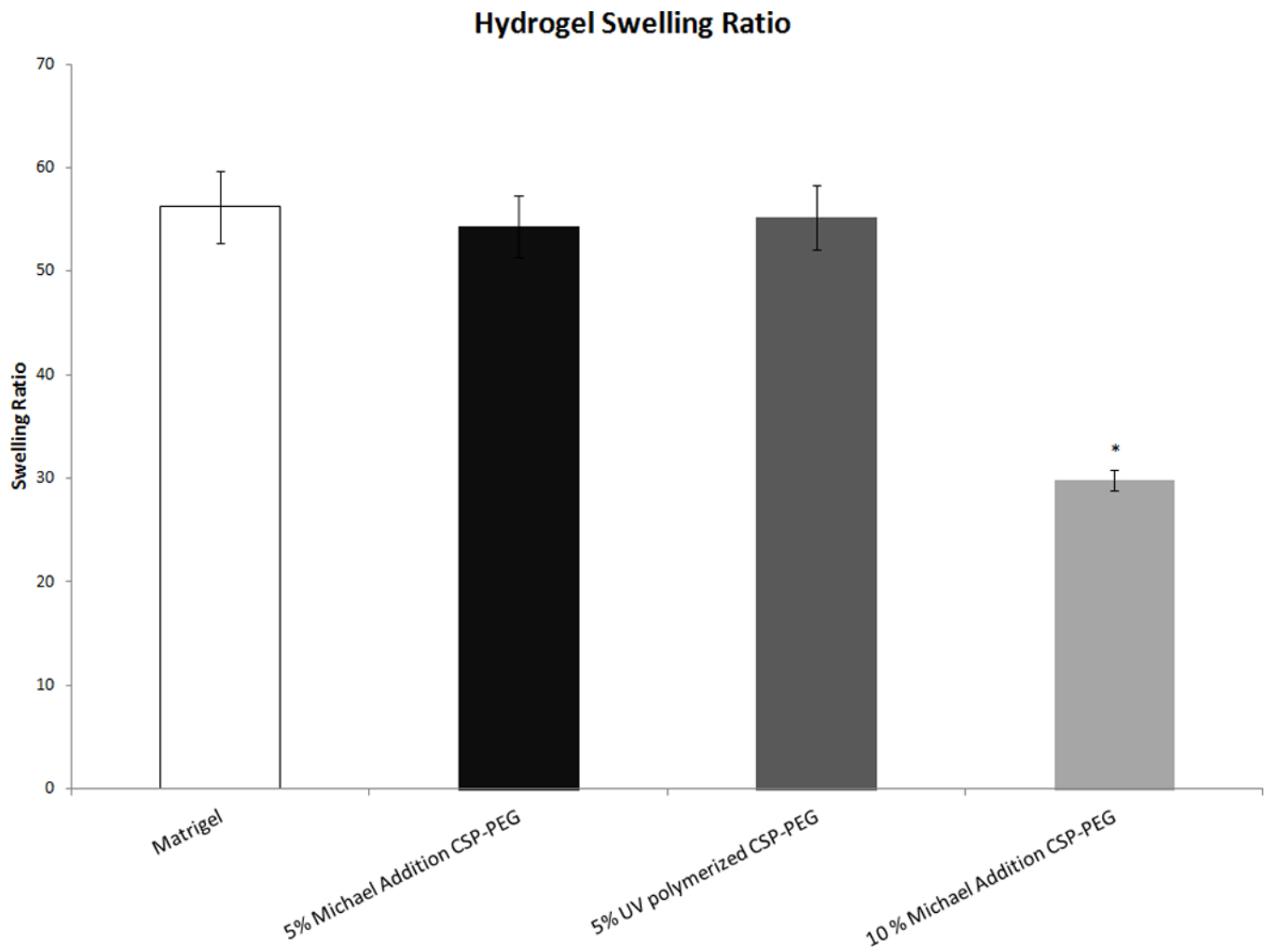


Figure 4. Average swelling ratios for four-arm CSP-PEG hydrogels (5% w/v) synthesized using Michael addition and UV polymerization as compared to both CSP-PEG (10% w/v) and Matrigel. Only the 10% w/v CSP-PEG hydrogel had a swelling ratio significantly different from Matrigel. *: $p < 0.05$ with regard to Matrigel.

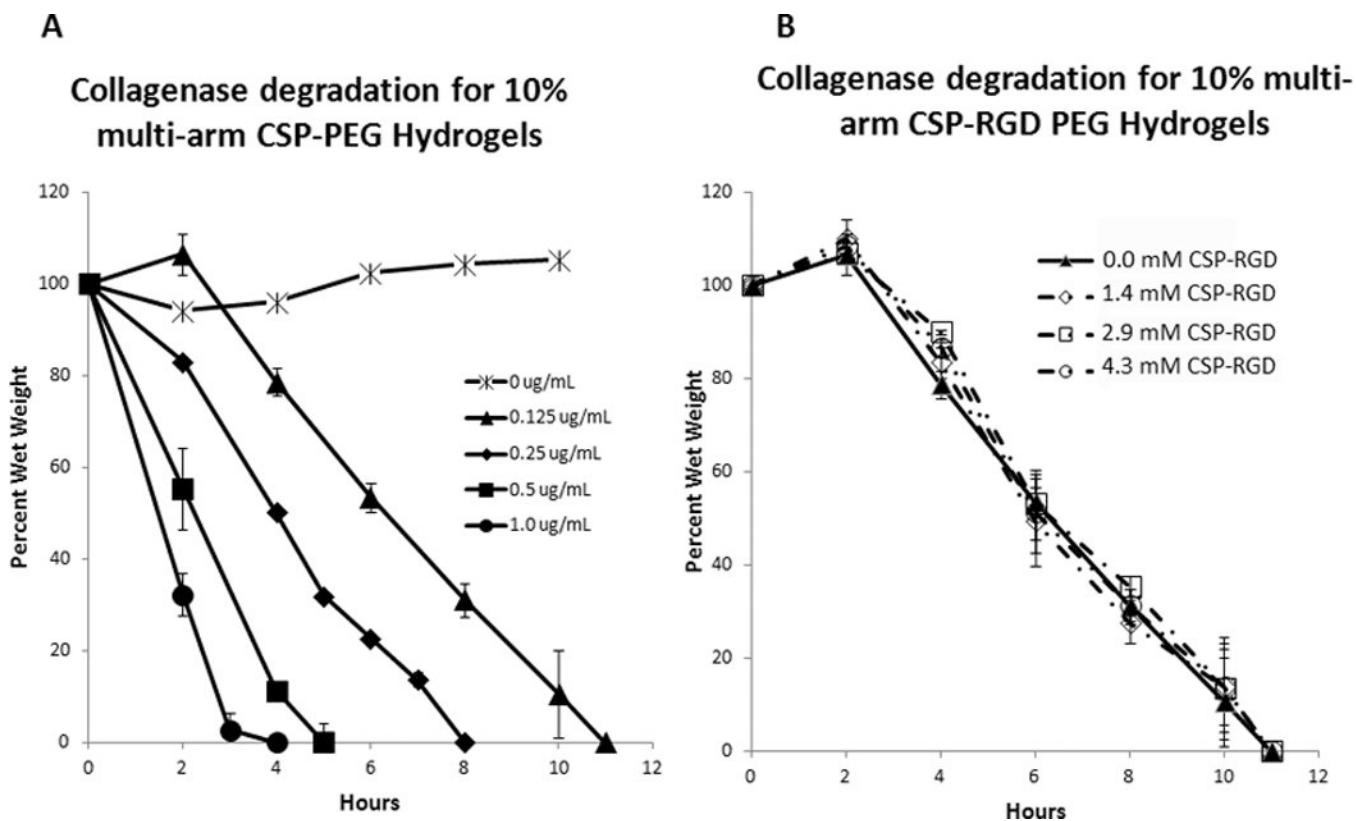
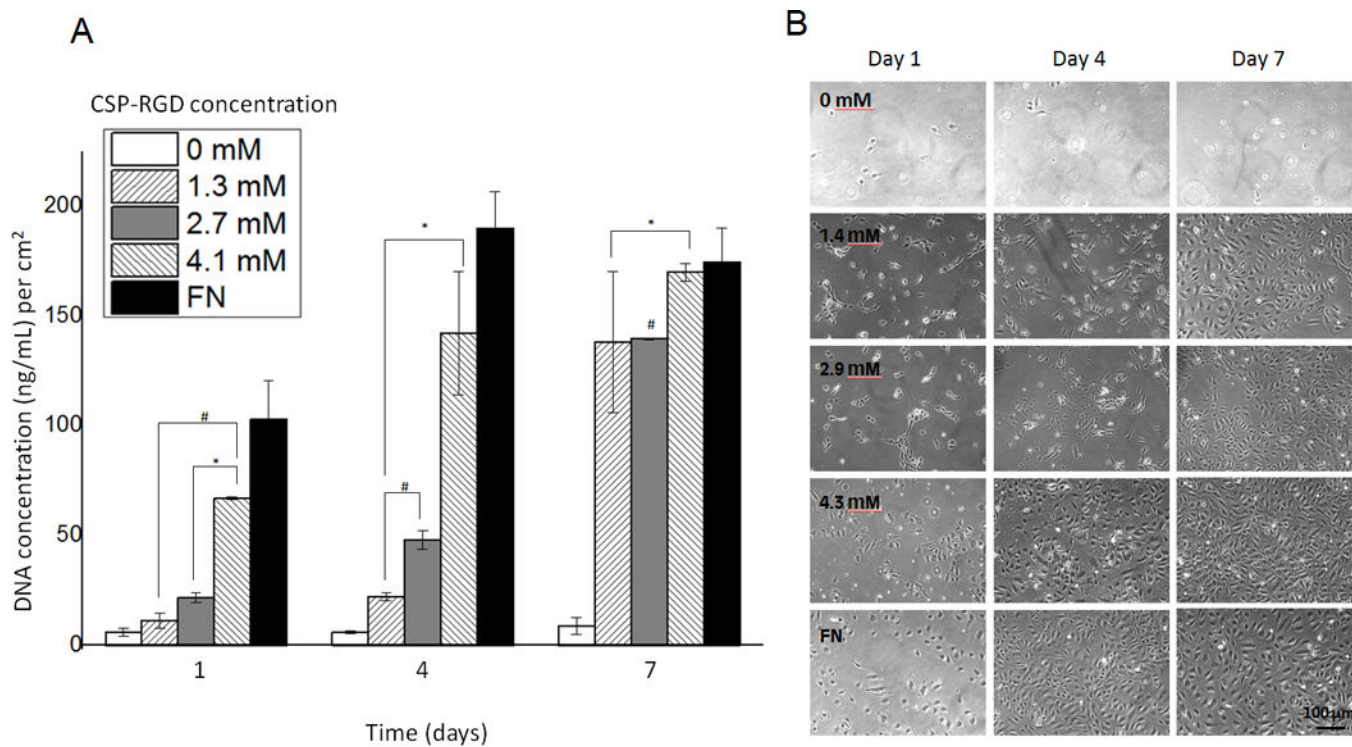


Figure 5.

(A) Degradation profiles of CSP-PEG hydrogels (10% w/v) in 0, 0.125, 0.25, 0.5, and 1.0 $\mu\text{g}/\text{mL}$ collagenase solution. Hydrogel degradation time decreased with an increase in collagenase concentration with hydrogels incubated in 1.0 $\mu\text{g}/\text{mL}$ collagenase solution degrading within 4 hours, 0.5 $\mu\text{g}/\text{mL}$ in 5 hours, 0.25 $\mu\text{g}/\text{mL}$ within 8 hours, 0.125 $\mu\text{g}/\text{mL}$ within 11 hours, and no significant change in mass for hydrogels incubated in 0 $\mu\text{g}/\text{mL}$ collagenase solution. (B) Degradation profiles for four-arm PEG acrylate hydrogels (10% w/v) with CSP-RGD concentrations of 0 mM, 1.4 mM, 2.9 mM, and 4.3 mM in 0.125 $\mu\text{g}/\text{mL}$ collagenase solution. There was no observable difference in the degradation profiles with respect to backbone linked RGD concentration, and all hydrogels degraded within 11 hours.

**Figure 6.**

(A) Cell proliferation four-arm PEG hydrogels (5% w/v) with CSP-RGD concentrations of 0.0 mM, 1.4 mM, 2.9 mM, 4.3 mM and a FN positive control surface. Picogreen assay was used to quantify the DNA concentration at 1, 4, and 7 day timepoints on functionalized hydrogels and fibronectin. (B) $10\times$ phase contrast images (1.5×10^4 cells/cm²) were taken for respective timepoints (scale bar = 100 μ m). *: $p<0.05$ with regard to DNA content with respect to CSP-PEG negative control at the same time point, #: $p<0.05$ with regard to DNA content with respect to FN positive control at the same time point.

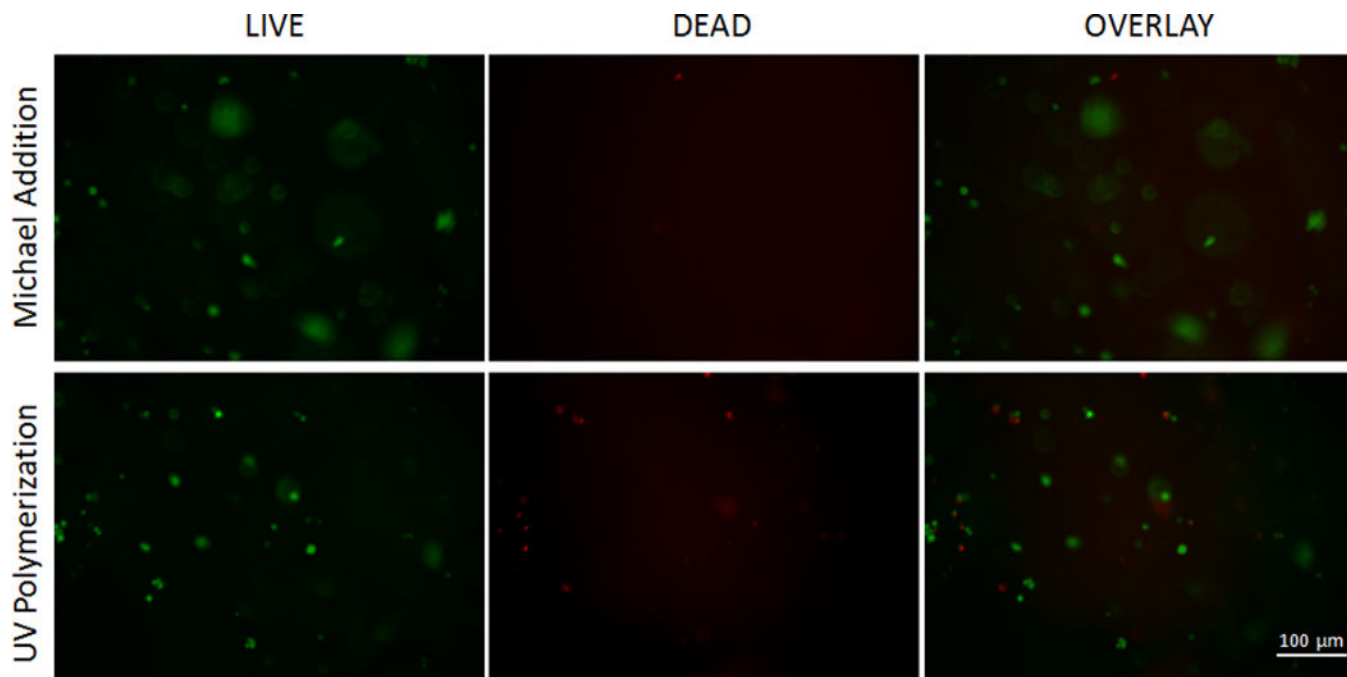


Figure 7. LIVE/DEAD assay for hydrogels synthesized by Michael Addition and UV polymerization. In the 10× images green fluorescence represents living cells stained by calcein and red fluorescence represents dead cells stained by EthD-1 homodimer. An average live cell percent of 80.9% was observed in hydrogels synthesized using Michael addition, and 52.1% for hydrogels synthesized using UV polymerization.